Licencia Creative Commons CC BY-NC-ND

EXPERIMENTAL AND NUMERICAL STUDY ON A FREEZE PROTECTION SYSTEM FOR FLAT-PLATE SOLAR COLLECTORS WITH SILICONE PEROXIDE TUBES.

Vera-Medina, J.[1], Lillo-Bravo,I.[2], Hernández, J. [2], Larrañeta M.[2]

[1] Solar Thermal Energy Department, National Renewable Energy Centre (CENER)

[2] Department of Energy Engineering, University of Seville

Corresponding author:

Jonathan Vera. National Renewable Energy Centre (CENER), C/ Isaac Newton, Nº4. Pabellón de Italia, 5ª Planta SO, 41092, Seville, Spain.

Phone number: (+34)948252800

E-mail: jvera@cener.com

Abstract

The freeze protection is essential in the majority of solar thermal installations to prevent breakage of solar thermal collectors. Therefore, there are different methods of protection against freezing of flat plate solar thermal collectors, all of them with certain limitations. This paper shows a novel freeze protection mechanism in the solar thermal collector by using flexible silicone peroxide tubes inside the absorber of the solar collector. We demonstrate, in a theoretical and experimental way, that the increase of volume and pressure produced inside a solar collector during freezing process can be absorbed using a flexible silicone peroxide tubes under all exposure conditions. The parameters that optimize the geometric configuration of the solution proposed have been calculated. A collector prototype with silicones peroxide has experimentally complied with the Standard ISO 9806:20 13, including freeze resistance test, without any significantly influence on its efficiency or pressure drop. Therefore, the solution proposed presents an inexpensive, effective, reliable and maintenance-free freeze protection system for flat plate solar collectors.

Keywords

Solar collector; freeze protection; silicone peroxide.

1 Introduction

The use of water in loop heat pipes is widespread due to it is high thermal performance, low cost and is non-toxic. Nevertheless, water has high expansion when cooled down to a sub-freezing temperature, leading to the breakage of the pipe [1-3].

Flat plate collectors are popular in low temperature heating applications and they are undergoing constant development in terms of size reduction, materials, efficiency and durability [4,5]. Flat-plate solar collector absorbers have selective surfaces that consist of a thin upper layer, which is highly absorbent to shortwave solar radiation but relatively transparent to longwave thermal radiation [6]. Therefore, the absorbers are made typically of good thermal conductors, mostly copper or aluminum, both are rigid. There are other materials, more flexible, used to a lesser extent such as EPDM, polypropylene, polyethylene or polymers, although their thermal conductivity and efficiency are low. These materials have the advantage of their low manufacturing cost and light weight [7-9].

The heat transfer fluid of a flat plate solar collector is typically water and in some applications air [10,11]. There are currently developments to improve the thermal conductivity of water adding nano-sized particles of high thermal conductivity like carbon or metals [12,13]. However, this does not prevent when the water contained in the absorber of a flat plate solar collector is frozen, its volume and pressure increases, which can lead to the breakage of the absorber. To avoid breakage of the absorber, different methods of freeze protection have been developed in flat-plate collector installations.

The main method used in the freeze protection is the addition of propylene glycol to the water circulating inside the absorber tubes of the solar collector [14-16]. However, this method´s main disadvantage is the degradation of the antifreeze with time as well as its high cost [17,18]. Other methods are:

- The recirculation of water in the collector loop [19,20] which requires forced circulation. This method can lead to a high-energy loss and, in some cases, may cause reliability problems if electric power is not available to activate the recirculation pumps at the required time.
- Recirculation in reverse flow [21]. This method can lead to a high-energy loss.
- The installation of an electric resistance along the tubes containing the water in the collector [22,23] but this can lead to high electricity consumption.
- Drain back system [24]. One of the main disadvantages of the drain back solar water heater is the significant source of the heat loss when the pump is not working, such as night exposure.
- The automatic drain-down of the installation [25]. These systems require of a special control and drained water cannot be recovered.
- There are other cases where the water storage and solar collector are on the same device in order to be always kept above the freezing temperature. For instance, this is the case of the system called Integrated Collector/Storage Solar Water Heaters, ICSSWH, based on a patented device in 1891 [26,27]. This method can lead to a high night energy loss.
- Other methods of protection with a solar heating system on two-phase using acetone or methanol as working fluid [28,29], but the thermal capacity is significantly reduced.

As described in the bibliography the different methods of protection have advantages and disadvantages. Bickle L. W. [30] proposed a method of protection based on introducing a flexible tube into the rigid tube of the absorber on the flat-plate solar collector. This method

was later patented [31], although the patent is now expired [32]. However, this reference and the patent indicated neither the characteristics of the material of flexible tube to be used nor the behavior of the proposed model in a real solar collector. Additionally, the study neither investigated the behavior of the flexible tube when the solar collector reaches high temperatures nor its influence on other characteristics of the solar collector (e.g. efficiency and pressure drop). Hence, the proposed system Bickle L. W. [30] had not been verified to comply with the current regulations.

In this paper, we propose a theoretical study complemented with an experimental validation of a flat plate solar thermal collector, which uses flexible silicone peroxide pipes, filled with air for a passive system of freeze protection compared with a commercial collector without flexible silicone peroxide pipes. Both collectors have been tested according to Standard ISO 9806:2013 (efficiency, freeze resistance, pressure drop and behavior at high temperatures tests).

Such method introduces a hollow flexible tube of external diameter D filled with air inside the tubes of the absorber of the solar collector, with internal diameter D_{rig}, so that the increase of volume produced in the freezing of the water, is compensated by the contraction of the air contained inside the silicone peroxide flexible tube located inside the pipe where the water circulates as shows in Fig. 1. The silicone peroxide tube must allow volume variation reliably and durably without any negative effect on the operation of the absorber.

Low cost and high durability under all operating conditions were the main criteria for selecting the flexible tube material. After the analysis of multiple materials, including different types of teflon and silicones, we propose the use of flexible silicone tube, and within this material, the silicone tubing blended with organic peroxide for its best performance against the platinum-cured silicone tubing, since it withstands higher temperatures and has a better physical compression capability.

Other advantages of silicone peroxide are the following: They have high resistance to compression deformation, non-toxic, weather resistant, ozone resistant, radiation and moisture resistant with the advantage of a relative low price. They are also suitable for food and sanitary use and therefore could be used in direct solar systems. The main drawback is the low resistance to vapors above 403 K. Table 1 shows its mechanical properties [33].

In addition, this freeze protection system could be used in other applications such as loop heat pipes or car radiators.

2 Theoretical model

This theoretical model determines the relationship between the diameters of the copper rigid pipe and the silicone peroxide flexible tube to allow absorbing the variations of volume and pressure during the process of freezing and overheating in a solar collector.

For this purpose, the thermal state equations of the different substances that intervene in the process have been used, imposing the limitations that the volume variation of the water in the freezing process inside the absorber is zero and that the maximum pressure achievable by the

rigid copper tube is lower than that supported by the copper tube during the freezing and heating process.

The geometric configuration of the whole new absorber tube is given by the parameter r_D which relates the inner diameter of the copper rigid pipe of the absorber, D_{rig} and the inner diameter of the silicone peroxide flexible tube $D(T_r, p_r)$ at reference condition (i.e. water at temperature T_r= 277 K and a pressure $p_r = 10^5$ Pa).

$$r_D = \frac{D_{rig}}{D(T_r, p_r)} \quad (1)$$

Parameter ε relates the diameter of the flexible tube at initial conditions (T_i, p_i) and at final conditions (T_f, p_f).

$$\varepsilon\,(T_i, p_i, T_f, p_f) = \frac{D(T_i, p_i) - D(T_f, p_f)}{D(T_i, p_i)} \quad (2)$$

Parameter r_v relates the volume of inner air of the flexible tube at initial conditions (T_i, p_i) and at final conditions (T_f, p_f).

$$r_V = \frac{V_a(T_i, p_i) - V_a(T_f, p_f)}{V_a(T_i, p_i)} \quad (3)$$

The relationship between the parameters r_D, r_v and ε is given by equations 9 and 10 and have been obtained as follows. It has been assumed that the thickness of the silicone flexible tube containing air is negligible.

The water volumes at the initial and final condition of the freezing process of the copper pipe are given by equations 4 and 5:

$$V_w(T_f, p_f) = \frac{\pi}{4} \cdot L_{tub} \cdot \left(D_{rig}^2 - D^2(T_f, p_f)\right) \quad (4)$$

$$V_w(T_i, p_i) = \frac{\pi}{4} \cdot L_{tub} \cdot \left(D_{rig}^2 - D^2(T_i, p_i)\right) \quad (5)$$

The variation of the water volume inside the copper pipe $\Delta V_w\,(T_i, p_i, T_f, p_f)$ depends on the variation of the specific volume of the water $\Delta v_{ew}(T_i, p_i, T_f, p_f)$ as shows in equation 6:

$$\Delta V_w(T_i, p_i, T_f, p_f) = m_w \cdot \Delta v_{ew}(T_i, p_i, T_f, p_f) = \rho_w(T_i, p_i) \cdot \frac{\pi}{4} \cdot L_{tub} \cdot \left(D_{rig}^2 - D^2(T_i, p_i)\right) \cdot \Delta v_{ew}(T_i, p_i, T_f, p_f) \quad (6)$$

The relationship between final and initial volume of water inside copper tube in freezing process is given by equation 7:

$$V_w(T_f, p_f) = V_w(T_i, p_i) + \Delta V_w\,(T_i, p_i, T_f, p_f) \quad (7)$$

Substituting equations (4) (5) (6) in (7) and clearing the diameter of the flexible tube at the final condition, $D(T_f, p_f)$ result equation 8

$$D(T_f, p_f) = \sqrt{D^2(T_i, p_i) \cdot \left(1 + \Delta v_{ew}(T_i, p_i, T_f, p_f) \cdot \rho_w(T_i, p_i)\right) - \Delta v_{ew}(T_i, p_i, T_f, p_f) \cdot \rho_w(T_i, p_i) \cdot D_{rig}^2} \quad (8)$$

The parameter ε is related to the parameters r_D and r_v defined according to expressions 1 and 3, through equations 2 and 8

$$\varepsilon = 1 - \sqrt{\left(1 + \Delta v_{ew}(T_i, p_i, T_f, p_f) \cdot \rho_w(T_i, p_i)\right) - \Delta v_{ew}(T_i, p_i, T_f, p_f) \cdot \rho_w(T_i, p_i) \cdot r_D^2} \quad (9)$$

$$r_V = 2\varepsilon - \varepsilon^2 \quad (10)$$

The behavior of the different substances, liquid water, ice, air and silicone, has been characterized by the state thermal equations in table 2.

Fig. 2 and Fig. 3 shows that by varying the temperatures of water and air from 273 K to 277 K the maximum increase in a specific volume of water occurs, outside these ranges the volume variation of the water is not significant and it´s behavior does not vary with the pressure. In the case of air, the variation of the air volume in that temperature range is very small and this variation does depend significantly on the pressure variation.

The increase of the diameters of copper and silicone tubes during the freezing process shows in Fig. 1, where increase of volume of water by freezing, $\Delta V_w\left(T_i, p_i, T_f, p_f\right)$ must be absorbed by a reduction of volume of flexible silicone with air inside, without reaching high-pressures on the whole. Therefore, this protection system does not prevent the freezing of the water but limits the maximum pressures that the solar collector reaches during its operation.

When $\varepsilon = 1$ the maximum contraction of the flexible tube is produced, also resulting in a value of $r_v = 1$ in these conditions. The maximum value achievable by r_D occurs when the largest volume increase of the water is reached in the freezing process, with $\varepsilon = 1$. According to Fig.2 is verified that the conditions of maximum variation of the volume of pure water happen practically when passing from T_i = 277 K; $p_i = 10^5$ Pa to T_f = 273.15 K; $p_f = 10^5$ Pa, resulting a maximum volume variation of water Δv_{ewmax} (277 K, 10^5 Pa, 273.15 K, 10^5 Pa) = 9.09 $\cdot 10^{-5}$ m^3/kg. Substituting this value together a density with $\rho_w(Ti, pi)$ = 999.97 kg/m^3, in equation 9, is obtained $r_{DMAX} = 3.45$.

In Fig. 4 shows the relationship between the three parameters, r_D, r_v and $\boldsymbol{\varepsilon}$.

If a value of r_D is too low, the volume of water available between the inner diameter of the silicone tube and the copper tube would be too small, and the water velocity would be very high, if it is desired to keep the mass flow rate of water in the absorber with great pressure drop. If a value of r_D is too close to the maximum value of 3.45, the air inside the flexible tube would exert a high pressure on the assembly and the copper tube may break, as shows in Fig. 4.

For the collector absorber to work properly, the variations of volume of the flexible tube with air on the inside in passing from initial condition T_i,p_i, which corresponds to the initial diameter $D(T_i, p_i)$, to the final condition T_f, p_f, which corresponds to the final diameter $D\left(T_f, p_f\right)$, must allow absorb the volume variations of the water inside the absorber tube when freezing, checking that the final pressure p_f is less than the maximum pressure supported by the rigid tube, thus preventing the absorber from breaking. This relationship between temperatures, pressures and geometry is determined by the equation 25 that has been deduced as follows:

Since it has been assumed that the copper tube of the absorber is rigid, $\Delta V_{rig} = 0$ being:

$$\Delta V_{rig} = \Delta V_w(T_i, p_i, T_f, p_f) + \Delta V_a(T_i, p_i, T_f, p_f) = 0 \quad (15)$$

Where

$$\Delta V_w = V_w(T_f, p_f) - V_w(T_i, p_i) \quad (16)$$

$$\Delta V_a = V_a(T_f, p_f) - V_a(T_i, p_i) \quad (17)$$

The equation above is an equation as a function of p and T.

$$m_w \cdot \Delta v_{ew}(T_i, p_i, T_f, p_f) + m_a \cdot \Delta v_{ea}(T_i, p_i, T_f, p_f) = 0 \quad (18)$$

Assuming there are no leaks, water mass m_w and air mass m_a keep constant and equal to those at the initial condition.

$$v_{ew}(T_i, p_i)^{-1} \cdot V_w(T_i, p_i) \cdot \Delta v_{ew}(T_i, p_i, T_f, p_f) + v_{ea}(T_i, p_i)^{-1} \cdot V_a(T_i, p_i) \cdot \Delta v_{ea}(T_i, p_i, T_f, p_f) = 0 \quad (19)$$

Dividing the above expression by the total volume of the inside of the pipe V_{rig}, it would remain that:

$$v_{ew}(T_i, p_i)^{-1} \cdot r_w(T_i, p_i) \cdot \Delta v_{ew}(T_i, p_i, T_f, p_f) + v_{ea}(T_i, p_i)^{-1} \cdot r_a(T_i, p_i) \cdot \Delta v_{ea}(T_i, p_i, T_f, p_f) = 0 \quad (20)$$

Where:

$$r_w(T_i, p_i) = \frac{V_w(T_i, p_i)}{V_{rig}} = \frac{A_w(T_i, p_i)}{A_{rig}} \quad (21)$$

$$r_a(T_i, p_i) = \frac{V_a(T_i, p_i)}{V_{rig}} = \frac{A_a(T_i, p_i)}{A_{rig}} = \left(\frac{D(T_i, p_i)}{D_{rig}}\right)^2 = \frac{1}{{r_D}^2} \quad (22)$$

$$r_w(T_i, p_i) = 1 - r_a(T_i, p_i) = 1 - \left(\frac{D(T_i, p_i)}{D_{rig}}\right)^2 = 1 - \frac{1}{{r_D}^2} \quad (23)$$

$$v_{ew}(T_i, p_i)^{-1} \cdot \left(1 - \left(\frac{D(T_i, p_i)}{D_{rig}}\right)^2\right) \cdot \Delta v_{ew}(T_i, p_i, T_f, p_f) + v_{ea}(T_i, p_i)^{-1} * \left(\frac{D(T_i, p_i)}{D_{rig}}\right)^2 * \Delta v_{ea}(T_i, p_i, T_f, p_f) = 0 \quad (24)$$

Equation 25 represents equation 24 after substituting D_{rig} from equation 1.

$$v_{ew}(T_i, p_i)^{-1} \cdot (1 - r_D^{-2}) \cdot \Delta v_{ew}(T_i, p_i, T_f, p_f) + v_{ea}(T_i, p_i)^{-1} \cdot r_D^{-2} \cdot \Delta v_{ea}(T_i, p_i, T_f, p_f) = 0 \quad (25)$$

Equation 25 relates the temperatures and pressures that are reached inside the copper tube from an initial condition at temperature T_i and pressure p_i to another final condition at temperature T_f and pressure p_f, according to geometry r_D, so that there is no volume variation in the rigid copper pipe. Subsequently it is verified that there is no rupture in the copper pipes and that the final pressure reached in the process p_f is less than the maximum pressure supported by the copper tube, p_{max}.

$p_f (T_i, p_i, r_D, T_f) < p_{max}$ (26)

3 Experimental analysis

Experimental analysis is aimed at testing two solar collectors according to Standard ISO 9806: a reference collector and a prototype one. Prototype collector is similar to reference one but where the silicone peroxide tubes are included and the tube of the absorber diameter is modified). The prototype collector has been designed according to the specific geometric parameters of r_D, r_V and ε determined according to the previous theoretical model. It is demonstrated that the prototype collector is able to pass all the tests and to withstand the freezing cycles. In addition, it is demonstrated that the influence of silicone flexible tubes on the energy performance and pressure drop of the collector is insignificant.

For the experimental analysis, a geometrical ratio has been taken in which the inner diameter of the absorber tubing is 8 mm and the inner diameter of silicone tube of 3 mm under initial conditions of 277 K and 10^5 Pa, which makes the value of $\mathrm{r_D}$ equal to $r_D = 2.67$, $\varepsilon = 0.31$ and $r_V = 0.53$ **.** This value of $\mathrm{r_D}$ is less than the permissible theoretical maximum of 3.45. In the calculations, the hypothesis of negligible the thickness of the silicone flexible tube was made.

Particularizing the equation 25 for geometry of $r_D = 2.67$, initial pressure p_i=10^5 Pa and initial temperature T_i= 273 K for the final temperatures between 278 K and 253 K, the final pressure is determinate, p_f. Figure 5 shown that the final pressure, p_f for different temperatures during the freezing process does not exceed to $3.3 \cdot 10^5$ Pa, well below the maximum pressure supported by the copper tube. Other represented geometry for different values of $\mathrm{r_D}$ and different pressures and temperatures can be analyzed for freezing processes.

Fig. 5 shows the configuration corresponding to the hollow flexible pipe is feasible according to the results of the model proposed for r_D=2.67.

Particularizing the equation 25 for geometry of $r_D = 2.67$, in overheating process, initial pressure p_i=10^5 Pa and initial temperature T_i= 315 K for the final temperatures between 315 K and 415 K, the final pressure is determinated by overheating process. Fig. 6 shows that the maximum final pressure does not exceed 3.8 10^5 Pa. Other geometries represented by different values of $\mathrm{r_D}$ and different values of pressures and temperatures can be analyzed for the overheating process.

For the experimental validation of the results, a commercial reference collector of *Termicol Energía Solar* brand (model T20MS), with an aperture area of 1.87m^2 has been used. It is a collector with an absorber type helix of 1.29 l and a copper tube of inside diameter 6 mm and thickness of 1 mm.

The manufactured prototype is identical to the previous one (same absorber surface, glass, absorber and posterior insulation) and a helix of the same length as that the commercial one has been placed but with copper pipe of inner diameter 8 mm and thickness 1 mm and a hollow silicone tube of inner diameter 3 mm and thickness 1 mm. This configuration means that the collector has a capacity of 1.24 liters (Fig. 7).

Both collectors have been testing according to Standard ISO 9806:2013 (Fig.8). The main tests to study are freeze resistance, efficiency, behavior at high temperatures and pressure drop tests.

From the point of view of costs, in the implementation of the prototype we used approximately 23 meter of flexible tube, which represents a ratio of 12.3 lineal meter/ m^2 of collector aperture area. The cost of the lineal meter has been 0.2 €, which has meant a collector total cost of 4.6 €. The reference collector has a cost of production of the order of 2.46 € / m^2 of collector aperture area. Taking into account this data, the cost of the proposed protection system is of the order of 3% the cost of the collector, with no maintenance costs.

3.1 Freeze resistance test

This is the main test for the object of the work and therefore the solar collector with the silicone peroxide tube inside was subjected to 20 freeze-thaw cycles according to section 15 of ISO 9806: 2013, with freezing temperatures between -20ºC ± 2ºC during 40 minutes and thaw condition to 15ºC ± 2ºC during 40 minutes, plus a rest time of 20 minutes. Fig. 9 shows a freeze-thaw cycle (T). The prototype passes the freeze resistance test satisfactorily.

3.2 Performance test

This test determines the performance curve of the collector, according to section 20 of ISO 9806:2013. The most common model of the performance of a thermal solar collector is well defined in this Standard as the dependence between the performance thermal η with respect to the global solar irradiance G, and the temperature difference between the average temperature of the fluid circulating in the collector t_m and the ambient air temperature t_a as follows:

$$\eta = \eta_0 - a_1 \cdot \frac{(t_m - t_a)}{G} - a_2 \cdot \frac{(t_m - t_a)^2}{G} \quad (27)$$

The average temperature of the fluid circulating in the collector is the average of inlet temperature t_{in} and outlet temperature t_e.

$$t_m = \frac{(t_{in} - t_e)}{2} \quad (28)$$

Fig. 10 show the performance curve of two tested collectors, the collector with inner silicone and reference collector.

The performance difference ($\Delta\eta_R$) is defined as:

$$\Delta\eta_R = \eta_{C.Ref} - \eta_{C.Sil} \quad (29)$$

Table 3 shows as the performance curve of both collectors has a maximum difference lower than 2%.

Table 4 shows the t-test calculation of the results obtained in Fig. 10. The p-value is 0.924. This value is greater than 0.05, so there is no statistical significant difference between the efficiency curves of the prototype and reference collectors.

Table 5 and table 6 shows the instantaneous efficiency curves, based on the aperture area, obtained to the reference collector and collector with inner silicone.

3.3 Exposure test

The exposure test provides operating conditions, which are likely to occur during real service, and allows the collector to “settle”, such that subsequent qualification tests are more likely to give repeatable results. Both collectors pass the exposure test satisfactorily for a class “A” test condition according to section 11 of ISO 9806:2013.

3.4 Pressure drop test across a collector

The biggest drawback of introducing a flexible pipe into the absorber tube is the increase in pressure drop. Fig. 11 shows the experimental values of the pressure drop in each collector are represented as a function of the water flow through the absorber, after testing both collectors according to section 28 of the Standard ISO 9806:2013.

The pressure drop across a collector (Δl_P) is defined as:

$$\Delta lp = C.P._{C.Sil} - C.P._{C.Ref} \quad (30)$$

Table 7 shows as the pressure drop between both collectors has a maximum difference lower than 9.5 kPa for these study flow.

Table 8 shows the t-test calculation of the results obtained in Fig. 11. The p-value is 0.715. This value is greater than 0.05, so there is no statistical significant difference between the pressure drop curves of the prototype and reference collectors.

Through this test, it is observed that the pressure drop increase with the flow is slightly higher in the case of collector with silicone tube. To overcome this drawback, the reference collector types should preferably be used in forced-circulations systems instead of thermosyphon, where the increase of the required energy to circulate the fluid due to the slight increase of the pressure drop would be contributed by the pump of the forced-circulation system.

4 Conclusions

It has been demonstrated theoretically and experimentally that the hollow flexible silicone peroxide tube prevent breaking the absorber tube absorbing water volume variations. In addition, it has been demonstrated that the solar collector with the flexible tube passes all durability tests according to the Standard ISO 9806:2013. Therefore, silicon peroxide tubes present an inexpensive, effective, reliable and maintenance-free freeze protection system, without any significantly influence on its efficiency or pressure drop.

This study showed that the performance of the proposed collector prototype (with silicone peroxide tube) is similar to the standard commercial collector. The efficiency and the pressure drop curves of the proposed collector prototype shows only minor deviations compared to the standard (reference) commercial collector.

Silicone peroxide has a low resistance to steam with temperatures above 403 K, this is considered as a limitation for the proposed system. Consequently, the proposed system is recommended to be installed in facilities with a controlled overheating process. In this sense, using forced circulation systems is favored over using thermosyphon systems, because the

differential control unit activates the overheating protection mechanism of the collector. Hence, once the temperature exceeds 403 K, the circulation pump may be activated to cool the collector.

5 Appreciations

Thanks to the Termicol, S.L. company for helping us in manufacturing the prototypes.

References

[1] C. Petit, B. Siedel, D. Gloriod, V. Sartre, F. Lefèvre, F. Bonjour. Adsorption-based antifreeze system for loop heat pipes. Applied Thermal Engineering 78 (2015) 704-711.

[2] Z. Wang, W. Yang, A review on loop heat pipe for use in solar water heating Energy Build. 79 (2014) 143-154.

[3] Yu F. Maydanik, M.A. Chernysheva, V.G. Pastukhov, Review: loop heat pipes with flat evaporators, Applied Thermal Engineering 67 (1) (2014) 294-307.

[4] S. A. kalogirou. Solar thermal collectors and applications. Progress in Energy and Combustion Science 30 (3) (2004) 231-295.

[5] B. Norton. Anatomy of a solar collector: Developments in Materials, Components and Efficiency Improvements in Solar Thermal Collector Systems. Refocus 7 (3) (2006) 32-355.

[6] J.A. Duffie, W.A. Beckman. Solar Engineering of Thermal Processes. John Wiley & Sons, Inc, New York, (1980).

[7] G. Martinopoulos, D. Missirlis, G. Tsilingiridis, K. Yakinthos, N. Kyriakis. CDF modeling of a polymer solar collector. Renewable Energy 35 (7) (2010) 1499-1508.

[8] J. Jyothi, H. Chaliyawala, G. Srinivas, H.S. Nagaraja, H. C. Barshilia. Design and fabrication of spectrally selective TiAlC/TiAlCN/TiAlSiCN/TiAlSiCO/TiAlSiO tandem absorber for high-temperature solar thermal power applications. Solar Energy Materials and Solar Cells 140 (2015) 209-216.

[9] D. Del Cola, A. Padovana, M. Bortolatoa, M. Dai Prèa , E. Zambolinb. Thermal performance of flat plate solar collectors with sheet-and-tube and roll-bond absorbers. Energy 58 (2013) 258-269

[10] S. Chamoli, R. Chauhan, N.S. Thakur, J.S. Saini. A review of the performance of double pass solar air heater. Renewable and Sustainable Energy Reviews 16 (2012) 481-492.

[11] A.A. Razak, Z.A.A. Majid, W.H. Azmi, M.H. Ruslan , Sh. Choobchian, G. Najafi , K. Sopian. Review on matrix thermal absorber designs for solar air collector. Renewable and Sustainable Energy Reviews 64 (2016) 682-693.

[12] M.A. Alima, Z. Abdin, R. Saidur, A. Hepbasli, M.A. Khairul, N.A. Rahim, A. Zamzamian, M. KeyanpourRad, M. KianiNeyestani, M. Tajik, J. Abad. Analyses of entropy generation and pressure drop for a conventional flat plate solar collector using different types of metal oxide nanofluids. Energy Build 66 (2013) 289-296.

[13] J. Jyothi, H. Chaliyawala, G. Srinivas, H.S. Nagaraja, H. Barshilia. An experimental study on the effect of Cu-synthesized/EG nano fluid on the efficiency of flat-plate solar collectors. Renewable Energy 71 (2014) 658-664.

[14] H. Imura, Y. Koito, M. Mochizuki, H. Fujiura. Start-up from the frozen state of two-phase thermosyphons. Applied Thermal Engineering 25 (17-18) (2005) 2730-2739.

[15] W. A. Beckman, J. Thornton, S. long. Control problems in solar domestic hot water systems. Solar Energy 53 (3) (1994) 233-236.

[16] O. Lottin, C. Epiard. Thermodynamic properties of some currently used water-antifreeze mixtures when used as ice slurries, Purdue University, International Refrigeration and Air Conditioning Conference, 2000.

[17] J. R. Clifton, W. J. Rossiter Jr., P.W. Brown. Degraded aqueous glycol solutions: pH values and the effects of common on suppressing pH decreases. Solar Energy Materials 12 (1985) 77-86.

[18] W. J. Rossiter Jr., MC Godette, P.W. Brown, K.G. Galuk. An investigation of the degradation of aqueous ethylene glycol and propylene glycol solutions using ion chromatography". Solar Energy Materials 11 (1985) 455-467.

[19] K.A. Laing, J.N. Laing. Freeze protection for hot water systems. US Patent US6622930 B2, 2003.

[20] K. Hudon, T. Merrigan, J. Burchand, J. Maguire. Low-cost solar water heating research and development roadmap. Technical Report NREL/TP-5500-54793, 2012.

[21] R. Tang, Z. Sun , Z. Li, Y. Yu, H. Zhong, C. Xia. Experimental investigation on thermal performance of flat plate collectors at night. Energy Conversion and Management 49 (10) (2008) 2642-2646.

[22] B. A. Wilcox, C.S. Barnaby. Freeze protection for flat-plate collectors using heating. Solar Energy 19 (6) (1977) 745-746.

[23] D.E. Prapas. Improving the Actual Performance of Thermosiphon Solar Water Heaters. Renewable Energy 6 (4) (1995) 399-406.

[24] R. Botpaev, Y. Louvet, B. Perers, S. Furbo, K. Vajen. Drainback solar thermal systems: a review." Solar Energy 128 (2016) 41-60.

[25] J. Burch, J. Salasovich. Water consumption from freeze protection valves for solar water heating systems. ISES Solar World Congress Orlando, Florida August 6-12, 2005. NREL/CP-550-37696.

[26] C. M. Kemp. Apparatus for utilizing the sun's rays for heating water. US Patent No. 451384. 1881-4-28, 1881.

[27] M. Smyth, P.C. Eames, B. Norton. Techno-economic appraisal of an integrated collector/storage solar water heater. Renewable Energy 29 (9) (2004) 1503-1514.

[28] A. Ordaz-Flores, O. García-Valladares, V.H. Gómez. Findings to improve the performance of a two-phase flat plate solar system, using acetone and methanol as working fluids. Solar Energy 86 (4) (2012) 1089-1098.

[29] E. Mathioulakis, V. Belessiotis. A new heat-pipe type solar domestic hot water system. Solar Energy 72 (1) (2002) 13-20.

[30] L. W. Bickle. Passive Freeze Protection for Solar Collectors. Solar Energy 17 (6) (1975) 373-374.

[31] E. Reed Stuart, R Tillman, W. Wahle Harold, O.H. Homeworth. Flexible insert for heat pipe freeze protection. Applied Thermal Engineering 17 (6) (1997) V-VI.

[32] http://documents.allpatents.com/l/18749894/US5579828A

[33] A. Colas, R. Malczewski, K. Ulman. Silicone Tubing for Pharmaceutical Processing. Dowcorning, 2004.

[34] J. S. Thomsen, T. J. Hartka. Strange Carnot cycles; thermodynamics of a system with a density extremum. Am. J. Phys.30 (1962) 26-33.

[35] J.J. Morgan, W. Stumm, J.D. Hem. Updated by Staff. Water. In: Anonymous Kirk-Othmer Encyclopedia of Chemical Technology: John Wiley & Sons, 2000.

[36] E.W. Lemmon, M.O. Mclinden, M.L. Huber. REFPROP Reference Fluid Thermodynamic and Transport Properties. NIST Standard Reference Database 23, Version 7.0, Physical and Chemical Properties Division ,2002.

[37] K. A. Waters. Properties of common engineering materials. ESDU DATA ITEM: ESDU 8041, 1984. Modify 2008.

FIGURES

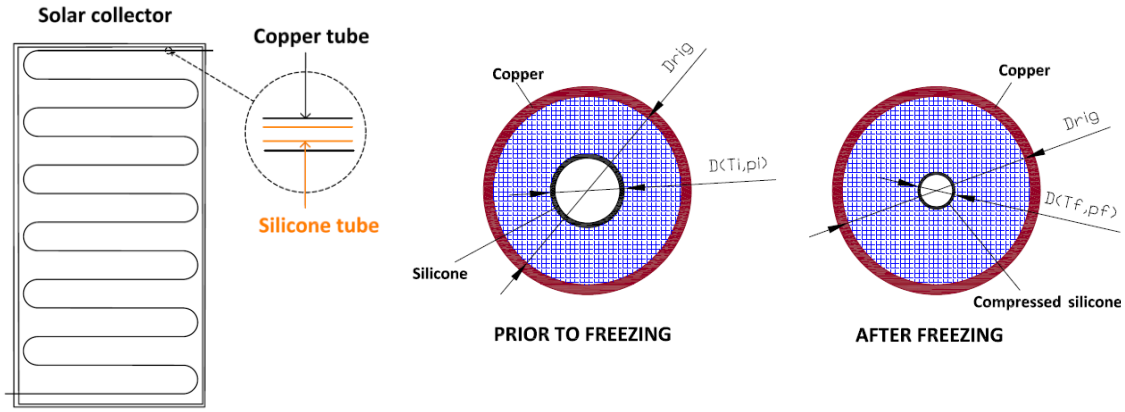

Fig 1. Collector with silicone tube.

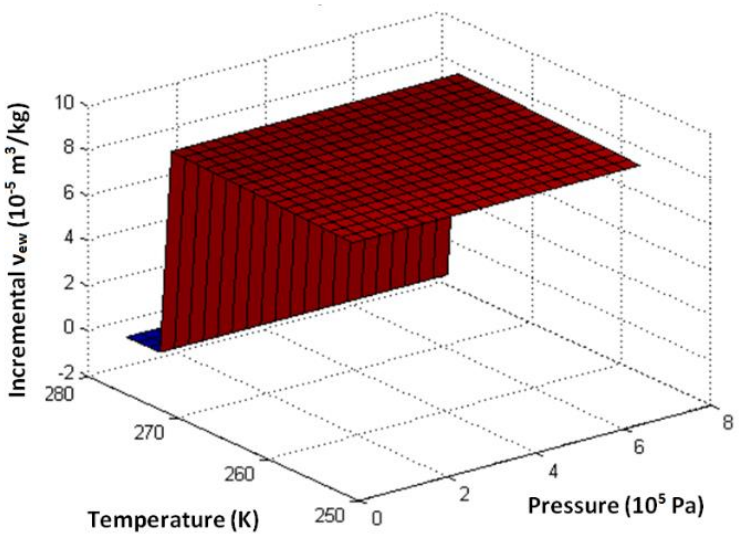

Fig 2. Incremental specific volume of water according to equations 11 and 12 of table 2

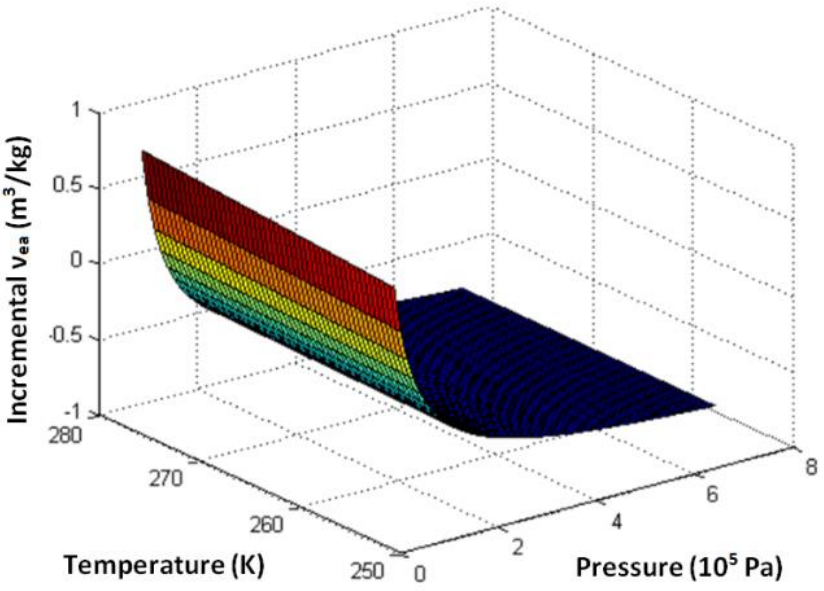

Fig 3. Incremental specific volume of air according to equation 13 of table 2

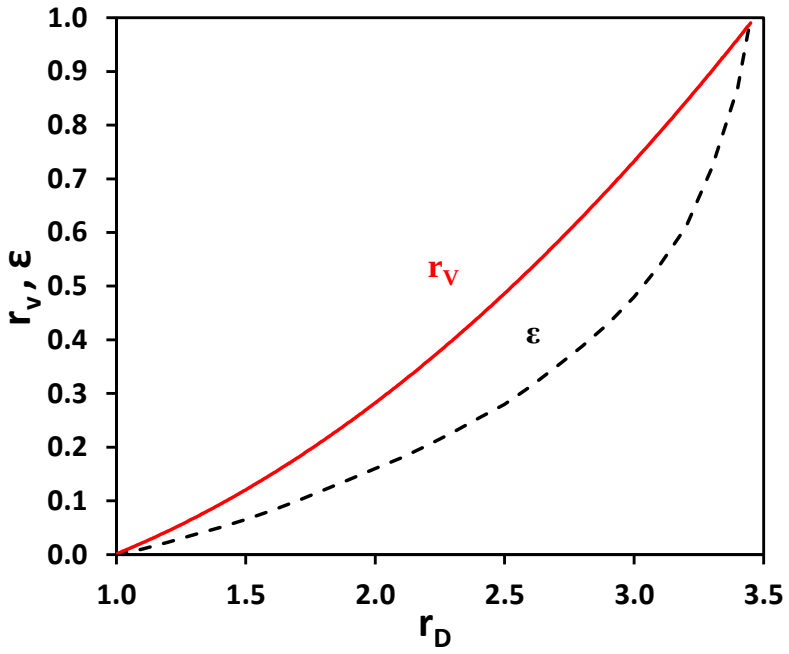

Fig 4. Variation of ε and r_V parameters for different r_D values

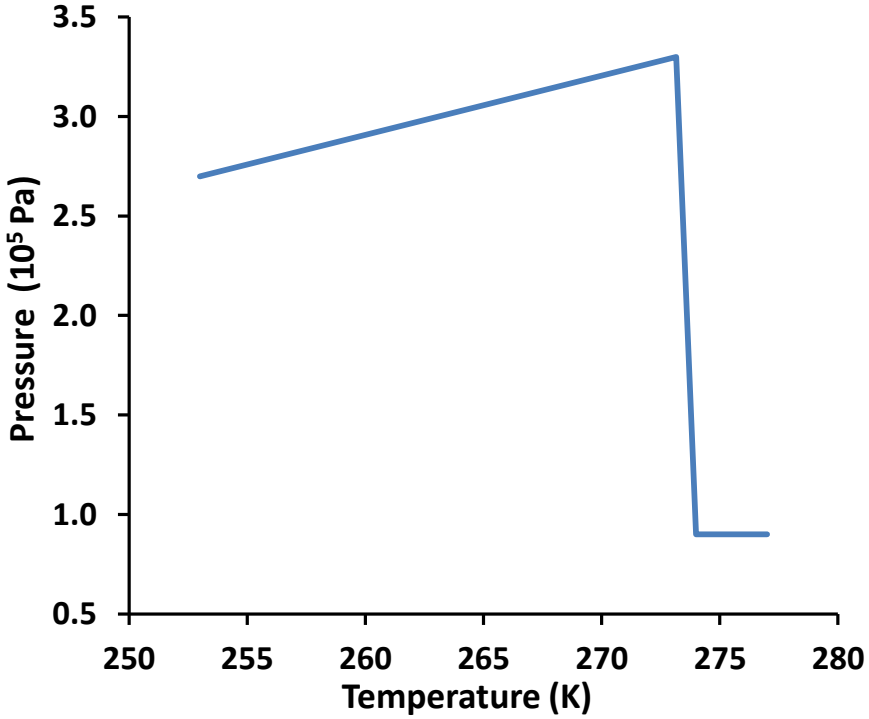

Fig 5. Final pressure that would reach the copper pipe as a function of the final temperature of water for values of T_i=273 K, p_i= 1bar and r_D=2.67.

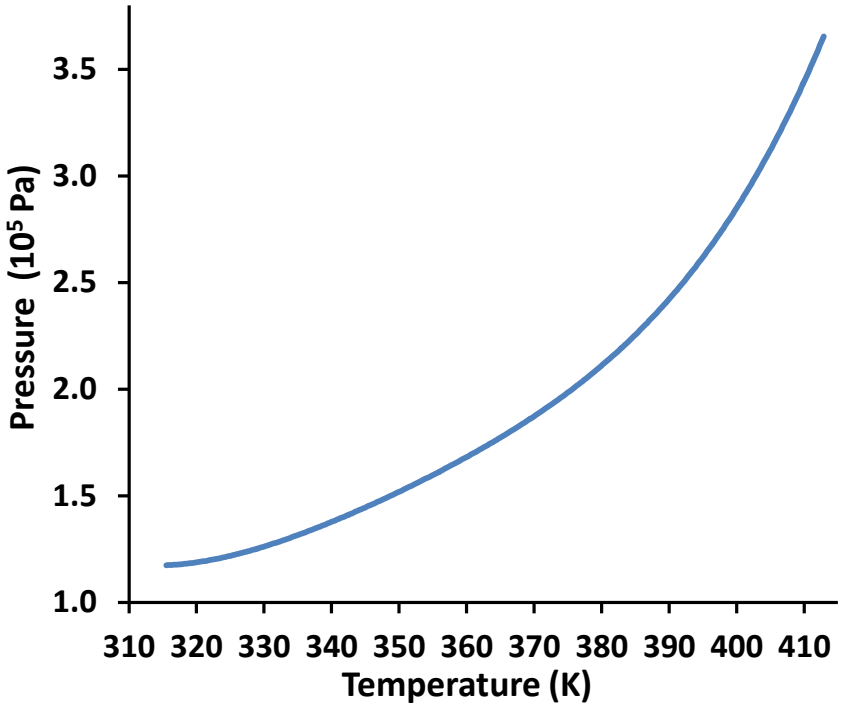

Fig 6. Water temperature and absorber tube pressure values reached.

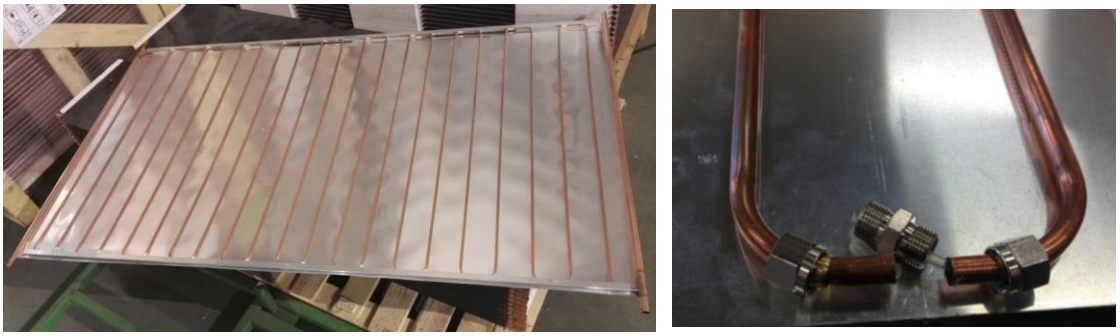

Fig 7. Collector absorber

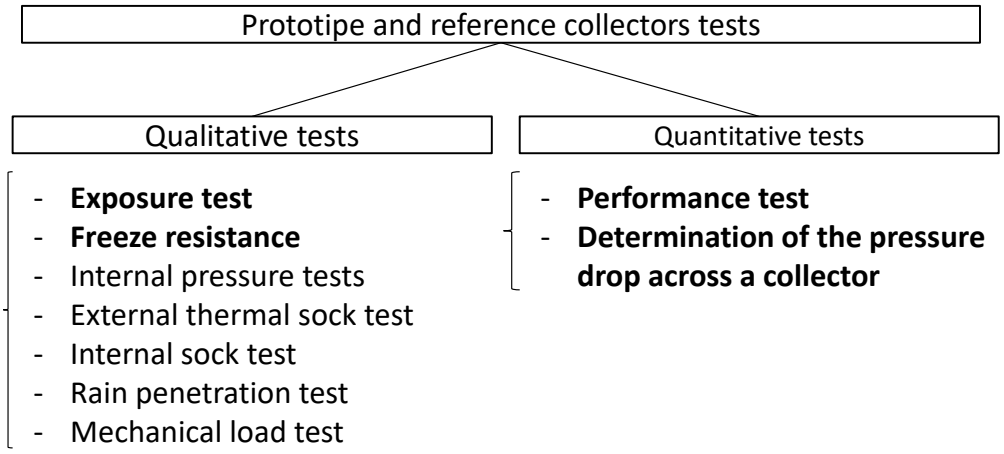

Fig 8. Flow diagram of the experimental validation (ISO 9806:2013)

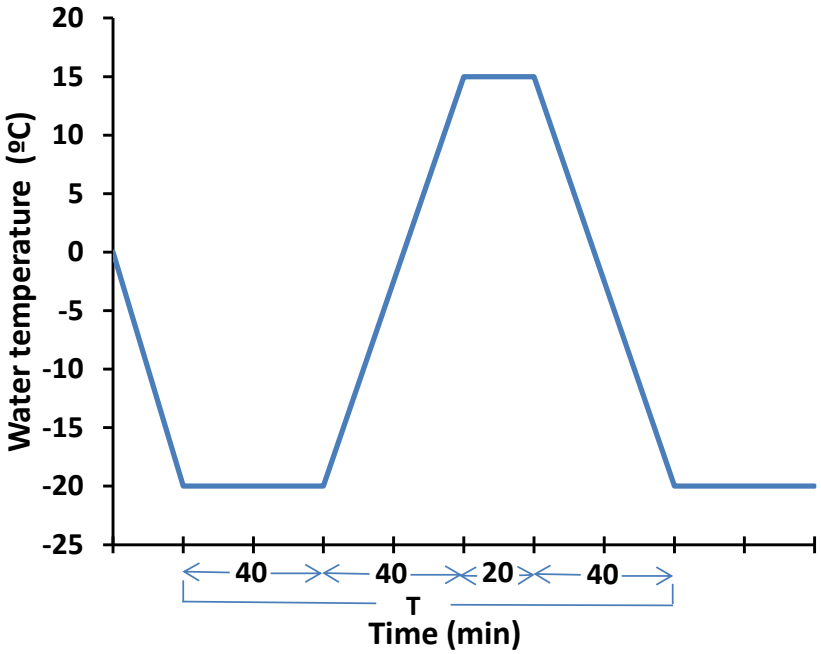

Fig 9. Exposure time of the absorber for a freeze-thaw cycle (T)

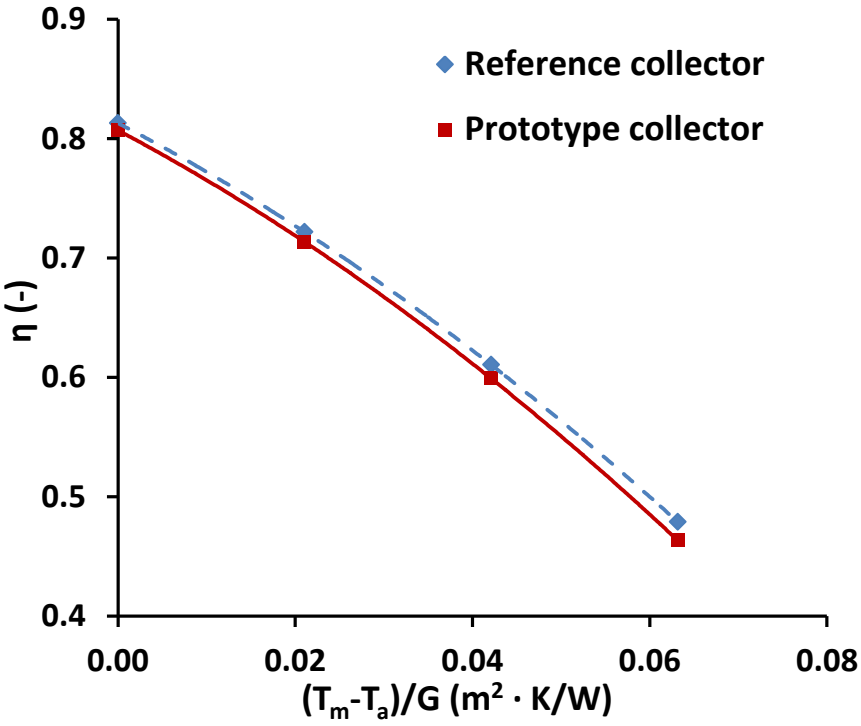

Fig 10. Adjustment of the quadratic efficiency curve with respect to the aperture area and average temperature of fluid for reference and prototype collectors

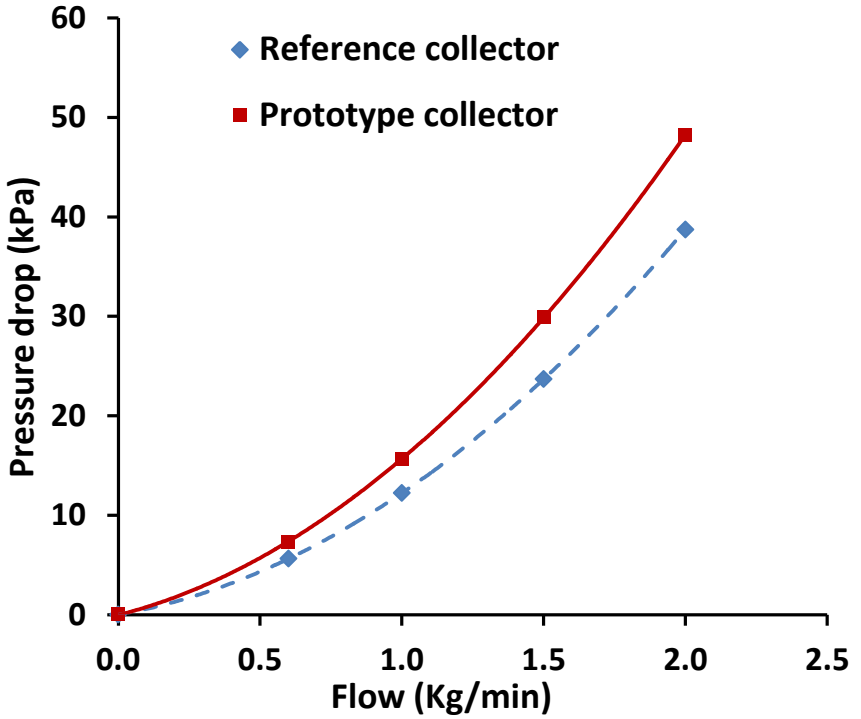

Fig 11. Pressure drop with respect of flow for reference and prototype collectors

TABLES

Table 1. Mechanical properties of silicone peroxide.

	Unit	Silicone
Tensile Strength	MPa	6.8-8.7
	psi	990-1265
Elongation at break	%	570-795
Hardness	Shore	A: 50-80
Brittle temperature	K	193
Max. Operating temperature	K	488

Table 2. Thermal equations of state used for liquid water, ice, silicone and air

Reference	Material	T-p range	Equations used	Parameters
[34]	Liquid water	273.15 – 288.15K 0.1 -10 MPa	$v_{ew}(T_f,p_f) = v_{e0cw}(1 + \lambda(T_f - T_{0w} + a\cdot p_f)^2 - k_0\cdot p_f$ (11)	$v_{e0cw} = 1.00008 \cdot 10^{-3}$ m^3/kg $\lambda = 8 \cdot 10^{-6}$ K^{-2} T_{0w}= 277 K $a = 2 \cdot 10^{-7}$ m s^2 K/kg $k_0 = 5 \cdot 10^{-10}$ m s^2/kg
[35]	Ice	150 K-273.15 K 0.1 -10 MPa	$v_{esol}(T_f,p_f) = v_{e0sol}\exp(\alpha_{Vsol}(T_f - T_{0sol}) - k_{Tsol}(p_f - p_{0sol}))$ (12)	$v_{e0sol} = 1.091 \cdot 10^{-3}$ m^3/kg $\alpha_{Vsol} = 171.6 \cdot 10^{-6}$ K^{-1} $k_{Tsol} = 0.12 \cdot 10^{-9}$ Pa^{-1} T_{0sol}= 273.3 K p_{0sol}= 101325 Pa
[36]	Air	59.75K-2000K 1-2000MPa	$v_{ea}(T_f,p_f)$ -> RefProp Program (13)	RefProp Program
[37]	Silicone	250 K-500K 0.05 -10 MPa	$v_{esil}(T_f,p_f) = v_{e0sil}\exp(\alpha_{Vsil}\cdot(T_f - T_{0sil}) - k_{Tsil}(p_f - p_{0sil}))$ (14)	$v_{e0sil} = 5.555 \cdot 10^{-4}$ m^3/kg $\alpha_{Vsil} = 1.71 \cdot 10^{-4}$ K^{-1} $k_{Tsil} = 2 \cdot 10^{-7}$ Pa^{-1} T_{0sil}= 273.3 K p_{0sil}= 101325 Pa

Table 3. Energy efficiency difference between reference and prototype collectors

T_m-T_a/G (m^2 · K/W)	0	0.021	0.042	0.063
$\Delta\eta_R$ (%)	0.600	0.832	1.147	1.547

Table 4. T-test of collectors' efficiency curve

T-test		
Parameter	**Reference collector efficiency curve**	**Prototype collector efficiency curve**
Median	0.656 (-)	0.646 (-)
Variance	0.021 (-)	0.022 (-)
Significance level	0.050	
Degrees of freedom	6.000	
t statistic	0.100	
p-value	0.924	
Critical value of t	2.447	

Table 5. Parameters of collector efficient curve with silicone peroxide

Collector with flexible tube			
Parameter	**Value**	**Standard deviation**	**Unit**
η_0	0.807	0.01	--
a_1	3.942	0.286	W/ $m^2 \cdot K$
a_2	0.025	0.002	W/ $(m^2 \cdot K^2)$

Table 6. Parameters of reference collector efficient curve

Reference collector			
Parameter	**Value**	**Standard deviation**	**Unit**
η_0	0.813	0.012	--
a_1	3.852	0.293	W/ $m^2 \cdot K$
a_2	0.024	0.002	W/ $(m^2 \cdot K^2)$

Table 7. Pressure drop difference, $\Delta \boldsymbol{lp}$

Flow rate (Kg/min)	0	0.6	1	1.5	2
$\Delta \boldsymbol{lp}$ **(kPa)**	--	1.7	3.4	6.3	9.5

Table 8. T-test of collectors´ pressure drop

T-test		
Parameter	**Reference collector pressure drop**	**Prototype collector pressure drop**
Median	16.052 (kPa)	20.227 (kPa)
Variance	238.452 (kPa)	368.884 (kPa)
Significance level	0.050	
Degrees of freedom	8.000	
t statistic	-0.379	
p-value	0.715	
Critical value of t	2.206	

Nomenclature

$A_a(T_i, p_i)\ (m^2)$ → Total area in any cross section to the axis of the cylinder occupied by the flexible tube at the initial condition

$A_{rig}\ (m^2)$ → Total area in any cross section to the axis of the inner cylinder to the rigid pipe at the initial condition

$A_w(T_f, p_f)(m^2)$ → Total area in any cross section to the axis of the cylinder occupied by the water at the initial condition

a_1 (W/(m^{2}K)) → Heat loss coefficient at (T_m-T_a) = 0

a_2 (W/(m^2 K^2) → Temperature dependence of the heat loss coefficient

C.P.$_{C,Sil}$ (kPa) → Pressure drop across the collector with flexible tube

C.P.$_{C,Ref}$ (kPa) → Pressure drop across the reference collector

$D\ (T_f, p_f)(\mathrm{m})$ → Inner diameter of the flexible tube at the final condition

$D(T_i, p_i)\ (\mathrm{m})$ → Inner diameter of the flexible tube at the initial condition

$D_{rig}\ (m)$ → Inner diameter of the copper tube

$\rho_W\ (T_i, p_i)(\mathrm{kg/m^3})$ → Water density at the initial condition

$L_{tub}(m)$ → Length of pipe

$m_w(\mathrm{kg})$ → Mass of water inside the rigid pipe

$m_a(\mathrm{kg})$ → Mass of air inside the silicone tube

$p_i(\mathrm{Pa})$ → Pressure at initial condition

$p_f(\mathrm{Pa})$ → Pressure at final condition

$r_a(T_i, p_i)$ → Ratio between initially air volume in the silicone flexible tube and total volume in the rigid pipe

r_{DMAX} → Maximum ratio between diameter of the rigid tube and diameter the silicone flexible inner tube during freezing process

$r_w(T_i, p_i)$ → Ratio between initially water volume and total volume of the rigid pipe

$T_i\ (\mathrm{K})$ → Temperature at initial condition

$T_f\ (\mathrm{K})$ → Temperature at final condition

$V_w\ (T_f, p_f)(m^3)$ → Volume of water under final temperature and pressure condition

$V_w\ (T_i, p_i)(m^3)$ → Volume of water under initial temperature and pressure condition

$v_{ea}(T_i, p_i)\ (\mathrm{m^3/kg})$ → Specific volume of air under initial temperature and pressure condition

$v_{ea}(T_f, p_f)\ (\mathrm{m^3/kg})$ → Specific volume of air under final temperature and pressure condition

$v_{esil}(T_f, p_f)(\mathrm{m^3/kg})$ → Specific volume of silicone at the final condition

$v_{esol}(T_f, p_f)(\mathrm{m^3/kg})$ → Specific volume of ice at the final condition

$v_{ew}(T_i, p_i)$ $(\mathrm{m}^3/\mathrm{kg})$ →. Specific volume of water under initial temperature and pressure condition

$v_{ew}(T_f, p_f)$ $(\mathrm{m}^3/\mathrm{kg})$ → Specific volume of water under final temperature and pressure condition

V_{rig} (m^3) → Inner volume of the rigid pipe

$V_a(T_i, p_i)$ (m^3) → Inner volume of air of silicone tube under initial temperature and pressure condition

$V_a(T_f, p_f)(\mathrm{m}^3)$ → Inner volume of air of silicone tube under final temperature and pressure condition

$V_w(T_i, p_i)$ (m^3) → Occupied volume by water under initial temperature and pressure condition

$V_w(T_f, p_f)$ (m^3) →. Occupied volume by water under final temperature and pressure condition

$\Delta V_w(T_i, p_i, T_f, p_f)(m^3)$ → Incremental volume of water (between the initial and final condition)

$\Delta V_{rig}(m^3)$ → Incremental volume inside of metallic rigid pipe

$\Delta V_a(T_i, p_i, T_f, p_f)(m^3)$ → Incremental volume of air inside the silicone tube (between the initial and final condition)

$\Delta v_{ewmax}(\mathrm{m}^3/\mathrm{kg})$ → Incremental maximum specific volume of water in the freezing process

$\Delta v_{ew}(T_i, p_i, T_f, p_f)(\mathrm{m}^3/\mathrm{kg})$ → Incremental specific volume of water (between the initial and final condition)

$\Delta v_{ea}(T_i, p_i, T_f, p_f)(\mathrm{m}^3/\mathrm{kg})$ → Specific volume increased of air inside the silicone tube (between initial and final condition)

η_0 → Zero-loss collector efficiency

$\eta_{c,Ref}$ → Efficiency of the reference collector

$\eta_{c,Sil}$ → Efficiency of collector with flexible tube